Journal of Renewable
Energy and Environment

Journal Homepage: www.jree.ir

MERC

Research Article

Study on Performance and Energy Balance of a U-Shape Flow Biomass Gasification System

Tsutomu Dei *a, Hossen Iddi Kayumba b, Julius Agaka Yusufu c

a Department of Engineering, Division of Mechanical Engineering, Ashikaga University, P. O. Box: 326-8558, Ashikaga, Tochigi, Japan.
b Tanzania Industrial Research and Development Organization, P. O. Box: 23235, Dar es Salaam, Tanzania.
c Energy Commission of Nigeria Headquarters, Garki, FCT-Abuja.

A B S T R A C T

This research explores biomass gasification for power generation in rural areas of developing countries, utilizing a 20 kW U-flow-shaped gasification system developed at Ashikaga University. While small-scale power systems typically rely on reciprocating or modified diesel engines, which face issues due to tar produced by biomass gasifiers, this study employed a piston-less rotary engine. Performance evaluations were conducted at various engine speeds and gasifier operational modes, demonstrating continuous power generation for approximately six hours. Improved maintenance of rotary engines could benefit rural users, with potential efficiency gains through thermal energy recovery, although tar filtration needs enhancement. The experimental findings reveal continuous power generation for approximately six hours under both operational conditions, with the closed-top operation outperforming the open-top counterpart in terms of power output. However, control over power output and gasifier temperatures is more straightforward in the open-top operation. Gasifier performance was assessed based on fuel consumption rate and system efficiency, with consumption rates varying by rotary engine speed, measuring 2.0 kWh/kg at 2800 rpm and 2.3 kWh/kg at 3200 rpm, and 2.9 kWh/kg at 3600 rpm. Cold gas efficiency of the U-shaped gasifier was 63.4%, and energy conversion efficiency reached 9.4% at 2800 rpm operation. At 3200 rpm operation, cold gas efficiency improved to 79.8%, but energy conversion efficiency decreased to 7.3%. The rotary engine's energy conversion efficiency was lower than that of a gas engine. Nonetheless, if the rotary engine reduces maintenance needs, it could benefit rural users. Efficiency can be improved through thermal energy recovery.

1. INTRODUCTION

The global population has increased 2.1-fold over the past 50 years, surpassing 8 billion in 2022. Projections suggest that the world's population will continue to grow, reaching an estimated 9.7 billion by 2050 (United Nations, 2022). This population growth is predominantly observed in developing countries, leading to various challenges such as heightened poverty and food shortages. It is anticipated that in the future, there will be an increased demand for energy, alongside issues related to water, food, and the environment. Particularly in developing nations, energy demands are escalating due to industrialization and improved living standards. Consequently, it is imperative to develop appropriate technologies that harness both conventional and renewable resources.

In sub-Saharan Africa, approximately 570 million people, constituting 46% of the regional population, lack access to electricity, with a notably low power utilization rate of 28.1%, especially in rural areas (REN21, 2021). Nearly 80% of renewable energy sources in developing countries are derived from biomass, primarily employed in inefficient traditional combustion methods (World Bioenergy Association, 2021).

Biomass energy assumes a crucial global role as a primary energy source. These resources are abundant in rural areas of developing countries but remain underutilized. Biomass is applied in various capacities in developing countries, encompassing electricity generation, thermal applications, and mechanical energy production (Garg & Sharma, 2013). However, most biomass resources are utilized for domestic purposes, such as cooking and heating, rather than for commercial purposes. Additionally, some traditional land use practices are unsustainable, depleting local soil nutrients, causing indoor pollution, posing health risks, increasing greenhouse gas (GHG) emissions, and potentially disrupting ecosystems if biomass is not replenished.

Despite some commercial usage, there is limited information available on the scale of these markets, including household fuel wood consumption in developed countries and the use of charcoal and fuelwood in developing nations (Shivpal et al., 2023). Multiple methods exist for generating energy carriers from biomass, with an analysis comparing three methodologies for biofuel production from energy crops: biogas, bioethanol, and biodiesel. The study highlights that the most energy-efficient method for generating energy is the

*Corresponding Author's Email: dei.tsutomu@g.ashikaga.ac.jp (T. Dei)
URL: https://www.jree.ir/article_193951.html

production of biogas from corn silage (Nikkhah et al., 2020). The primary technology for energy generation and heat provision involves the combustion and gasification of solid biomass resources. Ethanol production is the primary technology for fuel production in transportation. The production of ethanol involves the fermentation of sugar and starch crops. Exhaust emissions from diesel generators were investigated by supplying diesel and biodiesel blends in proportions of 10% and 15% (Adin et al., 2021). Furthermore, experiments involving blended fuel consisting of 20% biodiesel and 80% diesel by volume, along with n-butanol, led to decreased emissions of carbon monoxide (CO) and hydrocarbons in the exhaust gas (Şehmus et al., 2011). Among alcohol fuels, methanol was found to be more effective than ethanol in reducing CO emissions (Altun et al., 2023). Syngas is produced through the conversion of solid raw materials from biomass sources through gasification. Moreover, synthetic fuels such as high-quality diesel can also be produced from these feedstocks (Shivpal et al., 2023).

Biomass gasification represents a thermochemical procedure where solid biomass undergoes chemical conversion into gas when exposed to a gasification agent (Molino et al., 2018). The gasification process occurs within a range of temperatures from 750°C to 1300°C, utilizing agents including air, steam and oxygen or their combination. Gasification using air as the gasification agent is the most prevalent technology. Biomass feedstocks are combusted in the gasifier under controlled air supply conditions, primarily yielding syngas. Syngas consists of various flammable gases, including H_2, CO and CH_4, making it suitable for operating internal combustion engines to generate electricity (Toonssen et al., 2011). Air gasification is a straightforward, cost-effective, and reliable method. The supply of air enriched with oxygen and steam can enhance the content of flammable gases and heating value (Sittisun et al., 2019). However, the composition of the generated gas relies on factors like the type of gasifier, oxidizing agent, and operational parameters (Ayub et al., 2020).

Biomass energy represents a promising renewable energy source that can substitute for fossil fuels and reduce CO_2 emissions. Biomass's vast potential arises from its diverse range of raw materials and its adaptability to various alternative energy conversion pathways (Ibrahim et al., 2022). Numerous gasifier configurations exist worldwide, but they can be categorized into four primary categories: updraft, downdraft, fluidized bed, and entrained fluidized gasifiers (Chhiti et al., 2013).
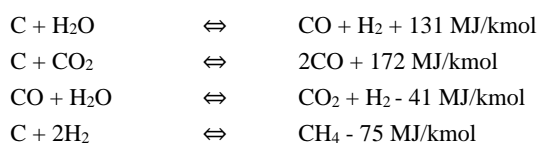
On Earth, a plethora of biomass resources of various species exist. The biomass resources can be classified into renewables and non-renewables categories. Renewable feedstocks include lignocellulosic biomass and municipal solid waste, among others. Woody and agricultural residues fall under the category of lignocellulosic biomass feedstocks, including sawdust, bark, and wood chips. Various agricultural residues, such as rice husk and bagasse, have been utilized as significant biomass feedstocks (Reddy & Vinu, 2018).

Fuel characterization typically involves both proximate and ultimate analyses, providing insights into fuel quality, suitability, and calorific value. Solid biomass can be evaluated by examining its moisture, ash, volatile matter, and fixed carbon contents, following the protocols established by the American Society for Testing and Materials. (Dhanak & Patel, 2016). During gasification, reduction processes yield flammable gases, including H_2, CO, and CH_4, at the reduction layer. The quality of char produced in the pyrolysis layer affects the composition of the output gas from the gasifier (Kushwah et al., 2022). Numerous factors influence gasification reactivity, such as the rate of temperature rise, temperature and pressure during pyrolysis, and the presence of inorganic components (Zeba et al., 2022). In the oxidation layer, biomass feedstock is burned with supplied oxygen from the air. Generally, air is continuously supplied as the agent to the gasifier. Several chemical reactions occur in this layer.

$$C + O_2 \quad \rightarrow \quad CO_2 - 394 \text{ MJ/kmol}$$
$$H_2 + 1/2O_2 \quad \rightarrow \quad H_2O - 242 \text{ MJ/kmol}$$
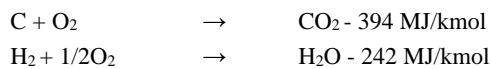
In the reduction layer, the temperature ranges from 800°C to 1100°C. The primary reaction is predominantly exothermic and endothermic. It can be described as follows.

$$C + H_2O \quad \Leftrightarrow \quad CO + H_2 + 131 \text{ MJ/kmol}$$
$$C + CO_2 \quad \Leftrightarrow \quad 2CO + 172 \text{ MJ/kmol}$$
$$CO + H_2O \quad \Leftrightarrow \quad CO_2 + H_2 - 41 \text{ MJ/kmol}$$
$$C + 2H_2 \quad \Leftrightarrow \quad CH_4 - 75 \text{ MJ/kmol}$$

There are two different configurations of downdraft gasifiers: one with a throat and one without. The former is known as the Imbert type, while the latter is referred to as the open-core type. The Imbert system involves a co-flow of gas and solid raw materials through the hearth zone, facilitated by a throat configuration. The downdraft gasifier has been successful in engine operation due to its low tar content (Reed & Das, 1988).

Power generation systems utilizing syngas produced by gasifiers offer the advantage of high-power generation efficiency, even in small capacities. Typically, modified reciprocating engines such as gasoline engines or modified diesel engines with ignition plugs are used in small-scale gasifiers. However, issues arise with tar production during the biomass gasification process. Tar tends to condense at lower temperatures, obstructing the flow of gas produced within connecting iron tube, filtering apparatus, and engines. Tar hampers the fluid motion of pistons in the engine.

The study explores a biomass gasifier connected to a rotary engine rather than a reciprocating engine. Additionally, the paper examines the operation of a generator powered by the gasification of woody biomass.

2. MATERIALS AND METHODS

2.1 Gasifier

Gasification is the process that transforms biomass feedstock into flammable syngas (Altun et al., 2023). Pyrolysis and gasification occur concurrently when the temperature rapidly increases during combustion. Consequently, the accumulation of high concentrations of volatiles is prohibited within the gasifier (Ibrahim & Mostafa, 2020). In an updraft-flow gasifier, as illustrated in Figure 1, the downward movement of biomass feedstock is accompanied by drying through the upward flow of syngas at elevated temperatures (Mishra & Upadhyay, 2021). The biomass feedstocks undergo pyrolysis in the upper section of the gasifier, where the thermal decomposition amidst elevated temperatures under the influence of atmospheric oxygen, resulting in their conversion into char, which continues to descend. Due to the limited

oxygen supply in reduction layer, the conversion process remains incomplete, leading to the formation of syngas, primarily composed of CO, H_2, CH_4 and other minor gases. Pyrolysis steam is generated within the gasifier and transported upwards by the high-temperature syngas flowing in the opposite direction (Kluska et al., 2018). The updraft gasifier represents a mature technology for heat production and is well-suited for small-scale applications.
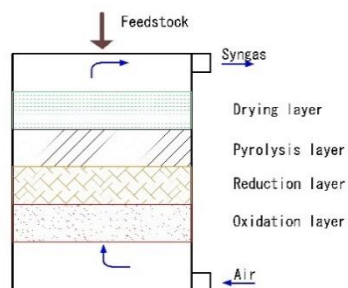

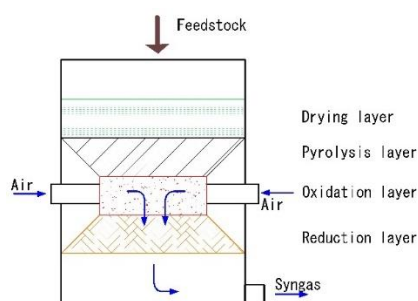**Figure 1.** Composition of updraft gasifier

Figure 2. Composition of downdraft gasifier

Regarding feedstock, the updraft gasifier can accommodate feedstocks with high moisture content, leaving minimal carbon residues in the ash. Additionally, direct heat exchange with the feedstocks enhances thermal efficiency. Another benefit of the updraft gasifier lies in its relatively reduced sensitivity to the ash generated within the gasifier. This is due to the fact that the highest temperature is reached near the ash discharge point located at the base of the reactor. Moreover, the updraft gasifier possesses a relatively simple structure and theoretically fewer scaling limitations (Carlos & Leonardo, 2020; Siedlecki et al., 2011). However, there is a size limitation for acceptable feedstock in updraft gasifiers due to the higher production of tar, necessitating extensive syngas cleanup before engine use. Furthermore, modifications are needed for the gasifier to remove ash from the outside, such as the installation of an auto-shaking mechanism for the grate. Addressing these issues is crucial, along with resolving problems related to the filters used to remove condensed tar.

Two distinct types of downdraft gasifiers exist: those with a throat and throat-less varieties. Gasifiers with throats are referred to as Imbert systems, while throat-less gasifiers are known as open-core types. In the Imbert system, gas and feedstocks flow in the same direction, moving downward through accumulated char, as depicted in Figure 2. Downdraft gasifiers have proven highly effective in engine operation due to their low tar content. Biomass feedstocks are introduced from the top of the gasifier and descend through drying and pyrolysis layers. Air is supplied from air intakes located at the top or sides of the gasifier. Within the gasifier, feedstocks and syngas move in parallel. Some of the feedstock is combusted

and then, descends through the grate to accumulate as a charcoal bed at the throat. The produced gases pass through this bed, resulting in the generation of high-quality syngas at the gasifier's bottom. Ashes present in the syngas are collected beneath the grate. In the drying layer, moisture evaporates from the biomass and slowly descends toward the pyrolysis layer. During the pyrolysis process, feedstocks are converted into char, tar, and syngas. Some of the pyrolysis products undergo combustion. Owing to the elevated temperatures within the pyrolysis layer, tars are cracked, leading to the generation of comparatively clean gas.

The furnace is a critical component of the gasifier. In the gasifier utilized in the experiment, air is introduced into the center of the gasifier via a pipe originating from the bottom. Biomass feedstock is supplied to the gasifier from the upper part, entering the drying layer. In this layer, water content in the feedstock vaporizes. Subsequently, the biomass feedstocks that have passed through the pyrolysis layer are transformed into char and volatile products. In the oxidation layer, volatile products undergo oxidation, while char is converted into syngas in the reduction layer (Branco et al., 2017; Ozgun et al., 2022). Gasifiers with downdraft airflow types produce syngas with low tar content. Therefore, they are particularly suitable for applications involving energy production by small engines. However, maintaining a consistent temperature within the gasifier using only the engine's airflow can be challenging. The gasifier produces more tar in the syngas as the internal temperature decreases. Conversely, at larger loads, the gasifier produces a smaller amount of tar due to increased airflow inside. If the load becomes excessively large, the tar production may increase again due to a shorter decomposition time.

The biomass power generation facility, consisting of a downdraft gasifier and a rotary engine, was designed by AU and used in the experiments (Dei & Iddi, 2021; Branco et al., 2017). Figure 3 illustrates the airflow inside the gasifier. Air is supplied through a pipe installed at the lower part of the gasifier, directed toward the center, and then flows downward through the reduction and oxidation layers. After passing through the grate and the gasifier's outer skirt, the airflow changes direction upward, defining a U-shaped flow pattern. The thickness of the drying layer varies with operational conditions, typically ranging from 100 to 400 mm, while the pyrolysis layer is approximately 100 mm thick, the oxidation layer is around 250 mm, and the reduction layer is roughly 100 mm. The gasifier's height is 2100 mm, and its diameter measures 930 mm. The inner furnace's volume is approximately 0.3 m³. To remove ashes or dust from the syngas and maintain the temperature at the gasifier's center, screw-shaped plates are welded along the inner part of the gasifier, as illustrated in Figure 4. The oxidation layer's temperature is recorded within the range of 700°C to 1,100°C, while the reduction layer's temperature is monitored between 600°C and 900°C. All experiments were conducted at atmospheric pressure. The biomass power generation system primarily consists of a downdraft and fixed-bed gasifier, along with temperature and airflow recorders, control systems, and measuring instruments, as shown in Figure 5, presenting the appearance of the biomass gasification system. Regarding feedstock, the updraft gasifier can accommodate feedstocks with high moisture content, leaving minimal carbon residues in the ash. Additionally, direct heat exchange with the feedstocks enhances thermal efficiency. Another benefit of the updraft gasifier lies in its relatively reduced sensitivity to the ash

generated within the gasifier. This is due to the fact that the highest temperature is reached near the ash discharge point located at the base of the reactor. Moreover, the updraft gasifier possesses a relatively simple structure and theoretically fewer scaling limitations (Carlos & Leonardo, 2020; Siedlecki et al., 2011). However, there is a size limitation for acceptable feedstock in updraft gasifiers due to the higher production of tar, necessitating extensive syngas cleanup before engine use. Furthermore, modifications are needed for the gasifier to remove ash from the outside, such as the installation of an auto-shaking mechanism for the grate. Addressing these issues is crucial, along with resolving problems related to the filters used to remove condensed tar.

Two distinct types of downdraft gasifiers exist: those with a throat and throat-less varieties. Gasifiers with throats are referred to as Imbert systems, while throat-less gasifiers are known as open-core types. In the Imbert system, gas and feedstocks flow in the same direction, moving downward through accumulated char, as depicted in Figure 2. Downdraft gasifiers have proven highly effective in engine operation due to their low tar content. Biomass feedstocks are introduced from the top of the gasifier and descend through drying and pyrolysis layers. Air is supplied from air intakes located at the top or sides of the gasifier. Within the gasifier, feedstocks and syngas move in parallel. Some of the feedstock is combusted and then, descends through the grate to accumulate as a charcoal bed at the throat. The produced gases pass through this bed, resulting in the generation of high-quality syngas at the gasifier's bottom. Ashes present in the syngas are collected beneath the grate. In the drying layer, moisture evaporates from the biomass and slowly descends toward the pyrolysis layer. During the pyrolysis process, feedstocks are converted into char, tar, and syngas. Some of the pyrolysis products undergo combustion. Owing to the elevated temperatures within the pyrolysis layer, tars are cracked, leading to the generation of comparatively clean gas.

The furnace is a critical component of the gasifier. In the gasifier utilized in the experiment, air is introduced into the center of the gasifier via a pipe originating from the bottom. Biomass feedstock is supplied to the gasifier from the upper part, entering the drying layer. In this layer, water content in the feedstock vaporizes. Subsequently, the biomass feedstocks that have passed through the pyrolysis layer are transformed into char and volatile products. In the oxidation layer, volatile products undergo oxidation, while char is converted into syngas in the reduction layer (Branco et al., 2017; Ozgun et al., 2022). Gasifiers with downdraft airflow types produce syngas with low tar content. Therefore, they are particularly suitable for applications involving energy production by small engines. However, maintaining a consistent temperature within the gasifier using only the engine's airflow can be challenging. The gasifier produces more tar in the syngas as the internal temperature decreases. Conversely, at larger loads, the gasifier produces a smaller amount of tar due to increased airflow inside. If the load becomes excessively large, the tar production may increase again due to a shorter decomposition time.

The biomass power generation facility, consisting of a downdraft gasifier and a rotary engine, was designed by AU and used in the experiments (Dei & Iddi, 2021; Branco et al., 2017). Figure 3 illustrates the airflow inside the gasifier. Air is supplied through a pipe installed at the lower part of the gasifier, directed toward the center, and then flows downward through the reduction and oxidation layers. After passing

through the grate and the gasifier's outer skirt, the airflow changes direction upward, defining a U-shaped flow pattern. The thickness of the drying layer varies with operational conditions, typically ranging from 100 to 400 mm, while the pyrolysis layer is approximately 100 mm thick, the oxidation layer is around 250 mm, and the reduction layer is roughly 100 mm. The gasifier's height is 2100 mm, and its diameter measures 930 mm. The inner furnace's volume is approximately 0.3 m³. To remove ashes or dust from the syngas and maintain the temperature at the gasifier's center, screw-shaped plates are welded along the inner part of the gasifier, as illustrated in Figure 4. The oxidation layer's temperature is recorded within the range of 700°C to 1,100°C, while the reduction layer's temperature is monitored between 600°C and 900°C. All experiments were conducted at atmospheric pressure. The biomass power generation system primarily consists of a downdraft and fixed-bed gasifier, along with temperature and airflow recorders, control systems, and measuring instruments, as shown in Figure 5, presenting the appearance of the biomass gasification system.
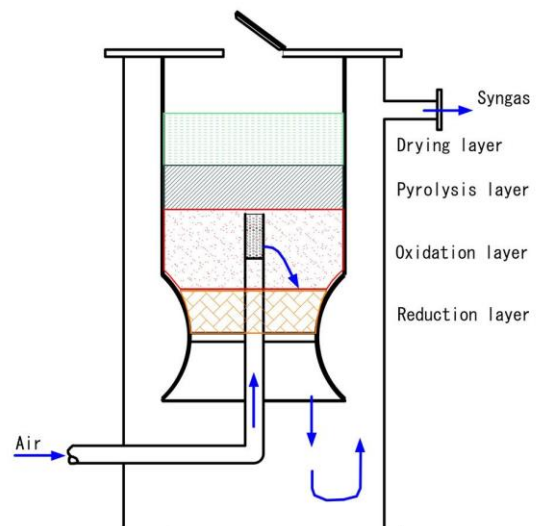

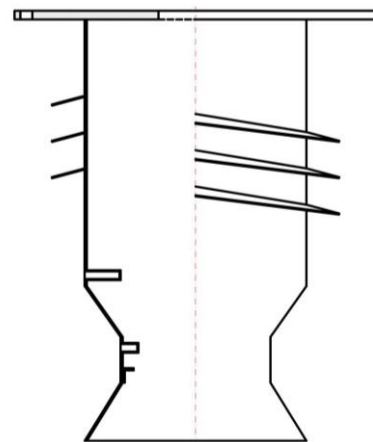**Figure 3.** Composition of U-shape flow gasifier

Figure 4. Screw-shaped plate around inner gasifier

Figure 5. Biomass gasification system

In a downdraft gasifier, the generated syngas flows downward and exits from the gasifier's bottom through an oxidation layer with a temperature of approximately 800°C. Consequently, a significant portion of the produced tar is consumed within the gasifier as the syngas traverses the oxidation layer.

During operation, biomass feedstock gradually descends under the influence of gravity, passing through sequential layers including the drying layer, pyrolysis layer, oxidation layer, and reduction layer. At the gasifier's lower section, syngas is generated through the gasification process. This produced gas is subsequently directed through filters, where it is mixed with air at a 1:1 ratio. The resulting gas-air mixture is supplied to a rotary engine, which in turn drives a synchronous generator. Figure 6 provides an illustration of the experimental facility's composition.
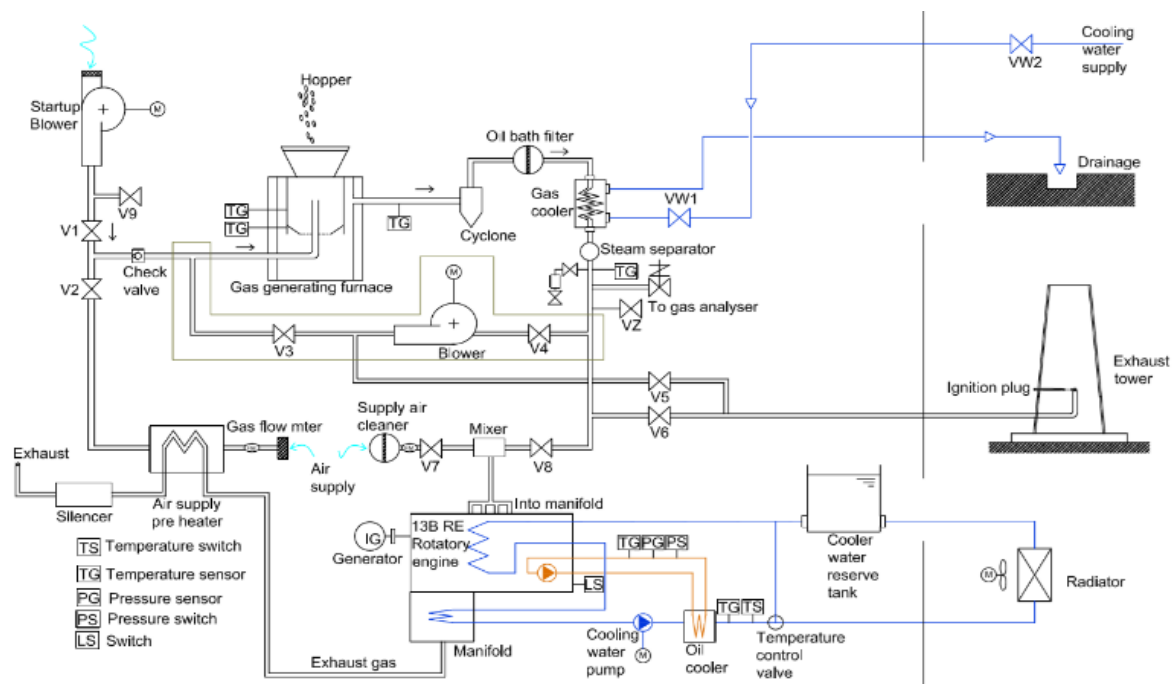

Figure 6. Schematic diagram of the pilot plant

2.2 Rotary Engine / Generator

In this study, Mazda's rotary engine was modified for experimental use. To mitigate the adverse effects of tar on the engine, the oil pan's volume of the oil pan was increased. Table 1 presents the specifications of the rotary engine and generator. The rotary engine underwent modifications to enable operation using the produced syngas. After removing moisture and certain materials, the produced gas is mixed with air through an air and gas mixer before being supplied to the internal engine. The engine's speed (rpm) is adjusted using an inverter. A rotary engine constitutes an internal combustion engine that incorporates triangular rotors within the housing. These rotors convert the pressure generated in the chambers during the combustion of fuel gas into kinetic energy. The engine comprises four distinct phases, with movements akin to reciprocating engines (Mazda Motor of America, 2020). The

advantages of combining a rotary engine with the biomass gasifier include its lightweight, compact design, and simplified structure compared to reciprocating engines. Rotary engines lack components such as crankshafts, valves, and rods, making them less mechanically complex. Typically, rotary engines have only three moving parts, enhancing their durability compared to reciprocating engines. Additionally, the unidirectional rotation of mechanical parts allows for operation at higher rotational speeds, facilitating the maintenance of low vibration levels. However, rotary engines have a primary drawback related to their lower thermal efficiency. This results in higher carbon emissions when compared to piston engines and reduced fuel efficiency. Another weak point of rotary engines lies in the rotors and apex sealings. Inadequate sealing between the rotors and the edges of the housing can lead to the leakage of combustion gases into adjacent chambers (Wankel, 2022).

Table 1. Specification of the engine and generator

Engine	
Engine Type and model)	Rotary Engine, 13B
Displacement	654 [cc] × 2 (2 rotor)
Compression ratio	9.7
Ratio (air vs. fuel)	1:1
Generator	
Rated power	20kW (3600rpm)
Type	2 pole 3 phases
Generated voltage	200V
Frequency	50Hz
Interconnection voltage	3 phases, 3 wire. 200V

2.3 Gas Analyzer

We used the same gas analyzer described in the studies of Dei & Iddi, 2021; Branco et al., 2017. The gasification system is linked to the gas analyzer as presented in Table 2. The analyzer monitors the composition of the generated syngas. The characteristics of the device are presented in Table 2.

Table 2. Specification of the gas analyzer

Manufacturer (Model)	Fuji Electric Systems Co., Ltd. (GASRACK-Z)	
Measurement range	CO_2	0 to 50(%)
	O_2	0 to 25/50 (%)
	CO	0 to 25/50(%)
	CH_4	0 to 5/20(%)
	H_2	0 to 30(%)
Repeatability	CO_2, CO, O_2, CH_4,	plus, or minus 0.5(%)
	H_2	plus, or minus 1.0(%)
Response	1 min	
Sampling method and volume	Dry sampling 3 to 6 litter/min	
Power source	AC 100V, 50Hz, 700 VA	

2.4 Procedure of power generation

Experiments were conducted using a 20-kW downdraft gasifier. Pieces of wood and charcoal served as feedstock for the experiment. Throughout the experiment, the temperatures in the oxidation and reduction layers, as well as the concentration of syngas, were continuously monitored. The gasifier's operation, the process began with ignited charcoal being introduced into the gasifier. Subsequently, air was supplied from the lower central part of the gasifier using a blower to elevate the internal temperature. Following this, feedstock was introduced into the gasifier at the desired feeding rate. Once the concentration of CO exceeded 15%, as indicated by the gas analyzer, the syngas was directed to the flare tower and ignited to confirm its combustibility. If it proved to be combustible, the syngas was then supplied to the rotary engine for power generation.

2.5 Biomass Feedstock

Biomass feedstocks are available in a wide range of sizes. Typically, the characterization analysis of biomass feedstocks includes both proximate analysis and ultimate analysis, along with an assessment of calorific value. These analyses provide insights into the quality of biomass feedstocks. Various feedstock characteristics, including specific surface areas,

forms, moisture content, volatiles, and carbon content, are recognized for their influence on gasification performance (Speight, 2015). For small-scale biomass gasification, it is convenient to operate the gasifier using well-prepared pellets or briquettes. Pellets or briquettes are compacted forms of biomass resources achieved through mechanical pressure, reducing their volume. These processed forms are more manageable than the original biomass resources.

3. RESULTS

3.1. Biomass Fuel

It is essential to investigate the characterization of biomass feedstock to determine their energy potential and optimize pyrolysis yields while minimizing environmental pollution during the pyrolysis process (Onokwai et al., 2022). In the experimental tests, plywood and laminated wood obtained as residue from an industrial company were utilized as biomass fuel. These biomass sources exhibited excellent performance for gasification due to the prior drying and compression during the industrial processes. Table 3 presents the results of proximate and ultimate analyses. The table's percentage values are presented on a dry weight basis, defined by Equation (1). M.Cwet denotes the moisture content of the substance, expressed as a percentage relative to its wet weight.

$$M.C_{wet} = \frac{Wet\ weight - Dry\ weight}{wet\ weight} \times 100\% \qquad (1)$$

The moisture content of the biomass fuel was low due to pre-drying during the industrial process. Plywood had a moisture content of 5.47%, while laminated wood had a moisture content of 1.88%. Plywood had a carbon content of 49.87%, and laminated wood had a carbon content of 83.91%. The hydrogen content for plywood was 6.25%, and for laminated wood, it was 6.28%. The size of the raw material varied as it was industrial residue, but it was approximately 800 mm × 800 mm × 200 mm in dimensions.

The heating value of the feedstocks represents the amount of heat released during continuous burning over a specific period. This value is expressed in energy units divided by substance units, such as kJ/kg, kJ/mol, kcal/kg, and Btu/lb. Biomass has a relatively low calorific value, particularly on a volumetric basis due to its low density. Heat quantity is measured by the heat generated when a unit quantity of the raw material is burned in a bomb calorimeter with oxygen. The calorific value reflects the heat content and considers the heat produced during the combustion of carbon, hydrogen, nitrogen, and sulfur in the feedstock. Calorific value is expressed as Higher Heating Value (HHV) and Lower Heating Value (LHV). In the HHV approach, the vapor produced during pyrolysis is condensed, while in the LHV approach, water content in the feedstock is removed by burning, and therefore not condensed. The HHV of the produced syngas was calculated using Equation (2), and the LHV was calculated using Equation (3) (Salam et al., 2022). HHV is influenced by ash, moisture, and oxygen content (Reddy & Vinu, 2018). The calorific values of the feedstocks used in the experiments were examined, resulting in an HHV of 4560 kcal/kg for plywood and 4830 kcal/kg for laminated wood. Table 3 presents the findings from the proximate and ultimate analyses, as well as the HHV. The ultimate analysis (C, H, N, S, O, Cl) is carried out following the JIS M8819 standard. The proximate analysis

of moisture and ash is performed according to JIS Z 7302-3 and 4, respectively, while volatile analysis follows JIS 8812. The higher heating value (HHV) is determined in accordance with JIS M7302-2.

$$HHV = 12.74\{H_2\} + 12.63\{CO\} + 39.82\{CH_4\} \ [MJ/m^3] \quad (2)$$
$$LHV = 10.78\{H_2\} + 12.63\{CO\} + 35.88\{CH_4\} \ [MJ/m^3] \quad (3)$$

Table 3. Ultimate and Proximate analysis of the feedstock

Analysis	Plywood	Laminated Wood
Moisture (wt%)	5.47	1.88
Ash (wt%)	2.54	0.28
Volatile (wt%)	75.68	83.91
C (wt%)	49.87	71.43
H (wt%)	6.25	6.28
N (wt%)	0.17	0.11
S (wt%)	<0.02	<0.02
O (wt%)	41.27	42.7
Cl (wt%)	0.02	42.7
HHV (kcal/kg)	4560	4830

3.2. Experiments

Figure 7 presents the outcomes of an experiment wherein the engine speed was set at 2800 rpm. The biomass gasifier methodically dispensed syngas for an uninterrupted duration of 270 minutes. During its operation, the gasifier effectively consumed 58.2 kg of woody biomass and an additional 25 kg of charcoal. Throughout the experiment, a controlled amount of 1.0 to 1.5 kg of woody biomass was introduced at five-minute intervals, and 0.5 to 1.5 kg of charcoal was introduced as needed, particularly when the gasifier's temperature fell below the desired threshold. The cumulative energy yield over the course of this operation amounted to 44.8 kWh. Within the gasifier, it is noteworthy that the mean temperature of the oxidation layer measured 867 °C, while the mean temperature within the reduction layer maintained at 746 °C during the entirety of its operation.

Figure 8 shows the outcomes of an experiment conducted with the engine speed set at 3200 rpm. The cumulative energy output from this operation was 70.2 kWh. The mean temperature of the oxidation layer was measured as 916 °C, while the mean temperature of the reduction layer was measured as 744 °C. Meanwhile, Figure 9 shows the results of an experiment conducted with the engine speed set at 3600 rpm. The cumulative energy output from this operation was 82.6 kWh. The mean temperature in the oxidation layer was measured as 844 °C, and the mean temperature in the reduction layer was noted as 721 °C.

As the engine speed increases, the intake air volume also increases accordingly. Consequently, the syngas produced in the gasifier becomes diluted and difficult to maintain at a suitable concentration for engine rotation. Fluctuations in engine rotational speed prompt alterations in the intake air volume, leading to subsequent fluctuations in the temperature within the gasifier. To maintain the temperature of the gasifier within a specific range, it is preferable to ensure automated and uninterrupted fuel supply. Alternatively, supplying fuel to the gasifier at brief intervals of 5 to 10 minutes while monitoring the temperature situation is considered advantageous.
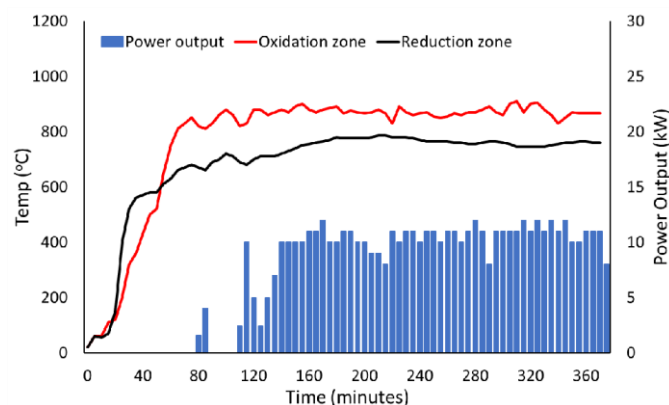

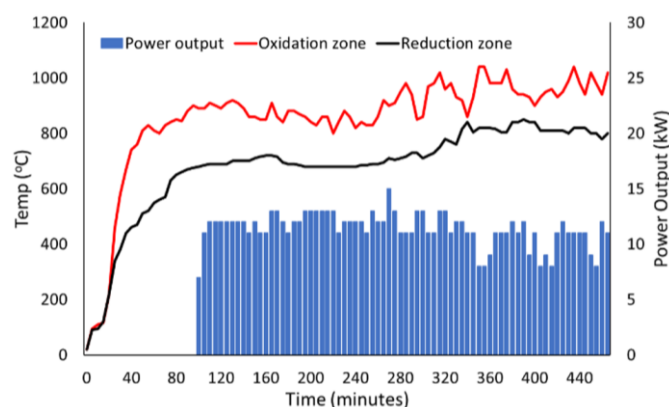**Figure 7.** Power output vs. temperature (open-top: 2800 rpm)
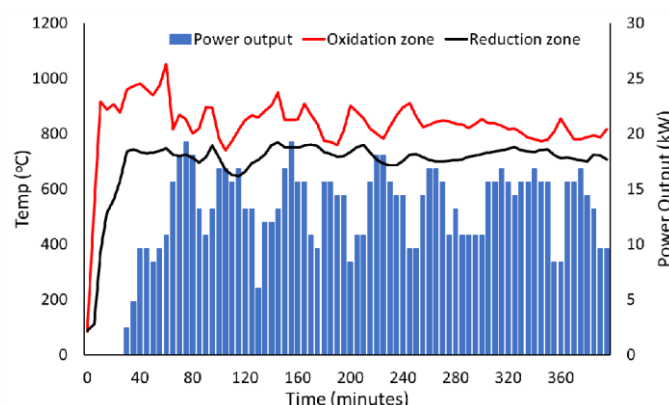

Figure 8. Power output vs. temperature (open-top: 3200 rpm)

Figure 9. Power output vs. temperature (close-top: 3600 rpm)

Table 4. Engine speed vs. Amount of consumed fuel

Proximate analysis				GCV		Ultimate analysis		
M %	VM %	Ash %	FC %	kcal/kg	MJ/kg	C %	H %	S %
5.7	79.1	0.7	14.3	4362	18.2	52	5.6	0.0

Table 4 elucidates the correlation between the engine's rotational speed within the rotary engine and the quantity of biomass fuel consumed to yield 1 kWh of energy. Evidently, as the engine's rotational speed escalates, there is a discernible augmentation in the volume of feedstock requisite for the generation of 1 kWh of energy.

3.3 Produced Gas

The experiment explored the dynamic behavior of gas components during the gasification process. Biomass gasification, a pivotal chemical reaction, regulates the

conversion of biomass feedstocks into a combustible gas, predominantly composed of CO and H_2. This intricate transformation is conventionally achieved by subjecting biomass feedstocks to a high-temperature environment, typically exceeding 700°C, while judiciously regulating the influx of air within the gasifier. The gasification process itself unfolds across four fundamental stages: heating and drying, pyrolysis, gas-solid reactions, and gas-phase reactions, as delineated by existing literature (Brown, et al., 2014). In the initial phase, the temperature within the heating and drying layer attains an approximate threshold of 300°C. Subsequently, within the second phase, one observes a rapid thermal decomposition of the biomass feedstocks transpiring within an anaerobic environment, characterizing the pyrolysis layer. The optimal temperature range for this thermal anaerobic decomposition hovers around 450°C. As the produced gas proceeds to the gas-phase reaction, two principal reactions come into play, namely, the water-gas shift reaction and methanation. Proximate and ultimate analyses were conducted under the auspices of the Tanzania Industrial Research and Development Organization (TIRDO). In accordance with ISO 1928:2009 standards, the calorific content was methodically ascertained. Biomass intended for thermal and electrical generation requires consideration of its higher heating value (HHV). The heating value serves as a metric for quantifying the energy content of a feedstock, measured using standardized methods. HHV specifically denotes the heat emitted during the complete combustion of a unit volume of the feedstock, resulting in the production and condensation of moisture vapor. In contrast, LHV does not account for this latent heat of water contained within the feedstock fuels (Voća et al., 2016). During the experiments, moisture content was assessed in accordance with ISO 589:2003 standards from the samples. Ash content was evaluated following ISO 1171:2010 protocols, while volatile matter content was determined in accordance with standard 562:2010. Ultimate analysis was conducted using a CHS analyzer (ELTRA CHS 580), and the energy content was determined using a Bob calorimeter (Parr 6100 Calorimeter). Table 5 succinctly presents summarized findings from both ultimate and proximate analyses of the biomass feedstock. It is noteworthy that the feedstocks underwent a drying process within a greenhouse, spanning a period exceeding six months, without any additional energy input for drying.

Table 5. Analysis of Robina pseudo acacia

Engine rotational speed of rotary engine	Amount of fuel for 1kWh production
2800 (rpm)	2.0 (kg/kWh)
3200 (rpm)	2.3 (kg/kWh)
3600 (rpm)	2.9 (kg/kWh)

The correlation between temperature and CO concentrations was investigated, as well as the relationship between temperature and power output during the operation of the biomass gasification system. This experiment was conducted with the gasifier's top lid open throughout the procedure. Additionally, the CO content produced by the downdraft gasifier during open-top operation was examined. In the experiment, a quantity of 4 kg of biomass solid fuel was gradually introduced every interval of 10 minutes, resulting in a total utilization of 36 kg of biomass solid fuel. The rotational speed of the rotary engine was set at 2800 revolutions per minute (rpm). The fluctuations in temperature within both the oxidation and reduction layers were carefully monitored and analyzed. While temperatures remained stable throughout the experiment, power output exhibited temporal instability. Remarkably, CO levels and power output displayed a similar variation pattern.

A parallel experiment was conducted with the gasifier's top lid closed to further explore the relationship between temperature and power output. Figure 10 illustrates the CO concentrations observed during open-top operation. In this experiment, 4 kg of biomass solid fuel was methodically introduced at 10-minute intervals, resulting in a total utilization of 40 kg of biomass solid fuel. The rotational speed of the rotary engine remained fixed at 2800 rpm. Comparative analysis of temperature profiles and power output revealed temporal fluctuations in power output. Notably, during closed-top operation, power output experienced a sharp decline when the top lid was opened for feedstock insertion. The average power output during closed-top operation surpassed that of open-top operation.
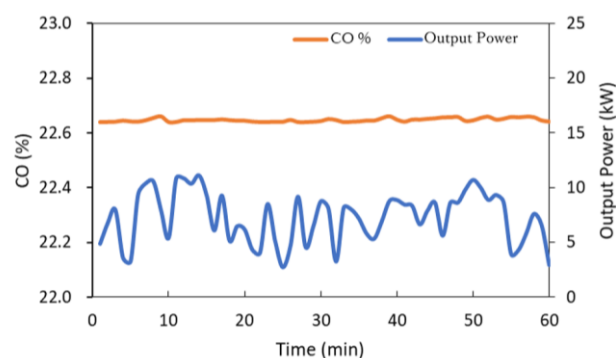

Figure 10. Power output and CO (open-top)

4. DISCUSSION

In this Chapter, the condition of the rotary engine after the experiments and the performance of the power generation system utilizing biomass gasifier is examined.

4.1. Rotary Engine

Rotary engines have recently garnered attention for their potential reliability as range extenders for electrically powered cars. Owing to their compact design, they deliver a superior power-to-weight ratio. Rotary engines offer distinct advantages in situations where space constraints necessitate compact engine installations, making them well-suited for deployment in small-scale power plants (Smail & Mohiuddin, 2020). Following the experiments, the rotary engine underwent periodic maintenance, during which tar residue was discovered inside the engine casing and deposited on the surface of the triangular rotor. It is imperative to enhance the filtering system, as the presence of tar within the engine could potentially lead to issues, particularly concerning the apex seal of the rotors (Dei & Iddi, 2021).

4.2. Cold gas efficiency

Cold gas efficiency measures how effectively a gasifier converts biomass into combustible gas without considering the energy used for the gasification process. Cold gas efficiency is calculated as follows (Murakami et al., 2013).

Cold gas efficiency (%) = (HHV in gasification gas (kJ/min))/(HHV of raw fuel (kJ/min))×100 (%)   (4)

The energy conversion efficiency reveals the ratio of energy content between desiccated raw materials and the energy output from the power generation system, as exemplified in Equation (5) (Bocci & Sisinni, 2020). This metric quantifies the efficiency with which desiccated raw materials are transformed into electricity. Gas engine is frequently employed in biomass gasification power plants, demonstrating an efficiency ranging from approximately 20% to 31% within the 4-25 kW power output range. Cold-gas efficiency and energy conversion efficiency of the U-shaped biomass gasification system are shown in Table 6 (Dei & Iddi, 2021). The cold gas efficiency of the similar capacity of a small-scale down-draft biomass gasification system, rated at 15 kW, is reported to be approximately 70% (Aguado et al, 2023). The cold gas efficiency of the U-shaped biomass gasification system at 2800 rpm is lower than that value, while at 3200 rpm it exceeds it. Table 6 indicates a decrease in energy conversion efficiency with increasing engine speed, implying that the gasifier's size may be inadequate to fully convert the supplied air into syngas. As the volume of intake air to the engine increased, the syngas produced in the gasifier became diluted. Consequently, the power output from the generator did not escalate proportionally with the increase in fuel consumption. It is imperative to explore and experiment with various combinations of U-shaped gasifiers and generators of different sizes to determine the optimal pairing of gasifier and engine.

$$Energy\ conversion\ efficiency = \frac{Generated\ Energy(kWh)}{Energy\ contents\ of\ dried\ feedstock\ (kWh)} \times 100(\%)$$ (5)

Table 6. Efficiency of biomass gasification

Engine rotational speed (RPM)	2800	3200
Cold-gas efficiency	0.634	0.798
Energy conversion efficiency	0.94	0.73

4.3. Efficiency of system utilization

In the biomass power station, the input energy comprises woody biomass, while the output energy is in the form of electricity. Energy efficiency quantifies the amount of energy extracted from the biomass resources by the biomass gasification power plant. This efficiency is defined as the ratio of the output energy to the input energy. Ideally, it is expected that "output energy / input energy > 1" should be achieved, with higher values indicating superior performance of the generation facility. The energy efficiency in this study is mathematically expressed by Equation (6).

$$Energy\ Efficienc = \frac{Total\ Power\ Generation\ (kWh)}{The\ sum\ of\ the\ input\ energy\ (kWh)} \times 100(\%)$$ (6)

During these experiments, woody biomass was sourced from a forest located approximately 30 km away from Ashikaga University (AU) and transported using a small utility vehicle. The forest exhibited a diverse array of tree species, resulting in a collection of wood materials representing a mixture of various tree types. To fell these trees, a chainsaw powered by a blended gasoline mixture was employed. The process of acquiring woody biomass from the forest involved not only fuel for the vehicle and chainsaw but also human labor, encompassing tasks such as biomass resource cultivation, post-growth logging, collection, unloading, and processing, among others. For calculation purposes, the energy expended in labor was estimated based on the typical energy consumption of a 70-kilogram adult male. Moreover, to ensure the operational functionality of the biomass power generation system, an allocation of electricity was necessary, primarily to sustain the operations of a blower, a cooling water pump, and a radiator fan. The residual wood ashes, which emerged as a byproduct of the process, have the potential to serve as valuable fertilizer, contributing to the cultivation of new biomass resources. The energy generated by the biomass power generation system represents the cumulative power output. Detailed insights into the energy efficiency of the system's utilization are presented in Table 7. Remarkably, the results indicate that the system achieved an impressive energy output, surpassing the input energy by a factor of 2.72. If the workload increases, operating costs will also rise accordingly. On the other hand, incorporating automated operation systems such as temperature control and fuel supply systems will lead to higher initial equipment costs. This research is aimed at introducing the system to developing regions such as the Sub-Saharan region; therefore, an automatic control system is not considered.

Table 7. Energy Efficiency of the System Utilization

Input(kWh)		Output(kWh)		Balance
Mixed gasoline (Chain saw)	3.12	Total generated energy	15.58	2.72
Labor	0.98			
Equipment (blower2 set / radiator fan / cooling water pump)	1.62			
Total	5.72	Total	15.58	

5. CONCLUSIONS

Obtained results indicate that the biomass gasification system, employing the U-shaped flow gasifier with a rotary engine and generator, can sustain power generation for approximately 6 hours continuously in both open-top and closed-top operations. Notably, the power output in the closed-top operation surpasses that of the open-top operation. Conversely, the control of power output and gasifier temperatures is more manageable in the open-top operation compared to the closed-top operation.

The performance of the U-shaped flow gasifier was assessed concerning the rate of fuel consumption and system efficiency. The rate of fuel consumption varied with the rotational speed of the rotary engine, measuring 2.0 kWh/kg and 2.3 kWh/kg at 2800 rpm, and 2.9 kWh/kg at 3200 rpm. It is evident that the amount of fuel consumed in producing 1 kWh increases with the rising engine rotational speed. At an operational speed of 2800 rpm, the cold gas efficiency reached 63.4%, with an energy conversion efficiency of 9.4%. In contrast, at 3200 rpm, the cold gas efficiency improved to 79.8%, but the energy conversion efficiency decreased to 7.3%. Notably, the cold gas efficiency improved with the increased rotational speed of the rotary engine. However, the efficiency of energy conversion worsens with an increase in engine speed. This phenomenon is attributed to the simultaneous increase in

the volume of intake air and feedstock consumption as the engine speed rises. Paradoxically, the increase in power generation is not proportional to the amount of consumed feedstock in the experiment. This discrepancy suggests an imbalance between gasification and combustion speeds at higher engine speeds. The pyrolysis reaction time shortened as the amount of supplied air increased, but the gasification reaction did not shorten significantly. This discrepancy is likely due to the relatively large size of the feedstock, which requires more time for complete gasification. To expedite the gasification reaction, smaller-sized feedstock such as pellets and small briquettes should be prepared.

The energy conversion efficiency of the biomass power system utilizing a rotary engine is lower compared to that of a gas engine. However, if the rotary engine can reduce maintenance burdens, it may prove beneficial for users in rural areas. The system's utilization efficiency stands at 2.72 and can be enhanced through the efficient recovery of thermal energy. Post-experiment analysis revealed the presence of tar in the rotary engine, highlighting the need for improvements in the filtering system.

6. ACKNOWLEDGEMENT

NOMENCLATURE

AU	Ashikaga University
C	Carbon
ºC	Celsius Degree
CH_4	Methane
CO	Carbon Monoxide
CO_2	Carbon Dioxide
FC	Fixed Carbon
GCV	Gross Calorific Value
GHG	Greenhouse Gas
H_2	Hydrogen
HHL	Higher Heating Value
kg	Kilogram
kmol	Kilomole
kW	Kilowatts
kWh	Kilowatts Hour
LHV	Lower Heating Value
M	Moisture
MJ	Mega Joule
Mm	Milli Meter
N	Nitrogen
rpm	Rotational Speed Per Minute
S	Sulfur
TIRDO	Tanzania Industrial Research and Development Organization
VM	Volatile Matter
wt%	Weight %

REFERENCES

1. Adin, M. Ş., Altun, Ş. & Adin, M.Ş. (2021). Effect of using bioethanol as fuel on start-up and warm-up exhaust emissions from a diesel power generator. International Journal of Ambient Energy, 43, 5711-5717. https://doi.org/10.1080/01430750.2021.1977387

2. Aguado,R., Escámez,A., Jurado,F., Vera,D. (2023). Experimental assessment of a pilot-scale gasification plant fueled with olive pomace pellets for combined power, heat and biochar production. Fuel, 344, 128127. https://doi.org/10.1016/j.fuel.2023.128127

3. Altun Ş, Adin M.Ş, İlçin K. (2023). Monohydric aliphatic alcohols as liquid fuels for using in internal combustion engines: A review. Proceedings of the Institution of Mechanical Engineers, Part E: Journal of Process Mechanical Engineering. https://doi:10.1177/09544089231160472

4. Ayub, H.M.U., Park, S. Jin., & Binns, M. (2020). Biomass to Syngas: Modified Stoichiometric Thermodynamic Models for Downdraft Biomass Gasification, Energies, 13(20), 5383. https://doi.org/10.3390/en13205383

5. Bocci, E., & Sisinni, M. (2014). State of Art of Small-Scale Biomass Gasification Power Systems: A Review of the Different Typologies. Energy Procedia, 45, 247-256. https://doi.org/10.1016/j.egypro.2014.01.027

6. Branco, J.P. Tamo, M.U.P., & Dei, T. (2017). Appropriate Feedstock in Wood Gasification for Rural Electrification. Energy Procedia, 138, 488-493. https://doi.org/10.1016/j.egypro.2017.10.232

7. Brown, R.C., & Brown T. (2014). BIORENEWABLE RESOOURCES: Engineering New Products from Agriculture 2nd edition, John Wiley & Sons, Inc. https://onlinelibrary.wiley.com/doi/book/10.1002/9781118524985

8. Carlos, A.D.G., Leonardo, P.S. (2020) Sustainable aspects of biomass gasification systems for small power generation. Renewable and Sustainable Energy Review, 134, 110180. https://doi.org/10.1016/j.rser.2020.110180

9. Chhiti, Y., & Kemiha, M. (2013). Thermal Conversion of Biomass, Pyrolysis and Gasification: A Review. The International Journal of Engineering and Science, 2(3), 75-85. https://www.theijes.com/papers/v2-i3/M023075085.pdf

10. Dei,T., & Iddi, H. (2021). Study on Biomass Gasified Generator Using Rotary Engine. Journal of Energy and Power Engineering 15, 187-192. https://doi.org/10.17265/1934-8975/2021.05.004

11. Dhanak, D.V., & Patel, V.R. (2016). Biomass Gasification: A Modern Approach for Renewable Energy Utilization, GRD Journal for Engineering, 1(6), 58-65. https://grdjournals.com/uploads/article/GRDJE/V01/I06/0066/GRDJEV01I060066.pdf

12. Garg, A., & Sharma, M. P. (2013). Performance Evaluation of Gasifier Engine System Using Different Feed Stocks. International Journal of Emerging Technology and Advanced Engineering, 3(6), 188-191. https://www.ijetae.com/files/Volume3Issue6/IJETAE_0613_31.pdf

13. Ibrahim, A., Veremieiey, S. & Gaskell, P.H. (2022). An advanced comprehensive thermochemical equilibrium model of a downdraft biomass gasifier, Renewable Energy, 194, 912-925. https://doi.org/10.1016/j.renene.2022.05.069

14. Ibrahim, S.M.A., & Mostafa, E.M. (2020). Syngas Compositions, Cold Gas and Carbon Conversion Efficiencies for Different Coal Gasification Processes and all Coal Ranks. Journal of Mining and Mechanical Engineering, 1(2), 59-72. https://10.32474/JOMME.2020.01.000109

15. Kluska, J., Ochnio, M., Kazimierski, P., & Kardaś, D. (2018). Comparison of downdraft and updraft gasification of biomass in a fixed bed reactor, Archives of thermodynamics 39 (4),59-69. https://journals.pan.pl/dlibra/publication/125656/edition/109645/content

16. Kushwah, A., Reina, T.R., & Short, M. (2022). Modelling approaches for biomass gasifiers: A comprehensive overview. Science of The Total Environment, 834, 15. https://doi.org/10.1016/j.scitotenv.2022.155243

17. Mazda Motor of America, Inc. Review (2020). RENESIS ROTARY ENGINE FUNDAMENTALS.https://www.academia.edu/42094967/Mazda_RENESIS_Rotary_Engine_Fundamentals

18. Mishra,S., Upadhyay, R. K. (2021). Review on biomass gasification: Gasifiers, gasifying mediums, and operational parameters. Materials Science for Energy Technologies, 4, 329-340. https://doi.org/10.1016/j.mset.2021.08.009

19. Molino, A., Larocca, V., Chianese, S., & Musmarra, D. (2018). Biofuels production by biomass gasification: A review. Energies, 11(4), 811. https://doi.org/10.3390/en11040811

20. Murakami, T, Asai, M., & Suzuki, Y. (2013). Optimized Approach of High Cold Gas Efficiency of Woody Biomass in a Fluidized Bed Gasifier with Triple-beds. The Japanese Society for Experimental Mechanics, 13 (special issue), 30-34. https://doi.org/10.11395/jjsem.13.s30

21. Nikkhah, A., El Haj Assad, M. Rosentrater, K. A., Ghnimi, S. & Van Haute, S. (2020). Comparative review of three approaches to biofuel production from energy crops as feedstock in a developing country. Bioresource Technology Reports, 10, 100412. https://doi.org/10.1016/j.biteb.2020.100412

22. Onokwai, A. O., Okokpujie, I. P., Ajisegiri, E. S., Oki, M., Adeoyeb, A. O., & Akinlabi, E. T. (2022). Characterization of Lignocellulosic Biomass Samples in Omu-Aran Metropolis, Kwara State, Nigeria, as Potential Fuel for Pyrolysis Yields. International Journal of Renewable Energy Development, 11(4), 973-981. https://doi.org/10.14710/ijred.2022.45549

23. Ozgun T. Nazlican K & Azize A (2022) Biomass gasification for Sustainable Energy Production: A Review: International journal of Hydrogen energy, 47(34), 15419-15433. https://doi.org/10.1016/j.ijhydene.2022.02.158

24. Reddy, B.R, & Vinu, R. (2018). Feedstock Characterization for Pyrolysis and Gasification. In S. De, A.V. Agarwal, V.S. Moholkar, & B. Thallada (Eds.), Coal and Biomass Gasification: Feedstock Characterization for Pyrolysis and Gasification (pp.37 -62). Springer. https://doi.org/10.1007/978-981-10-7335-9_1

25. Reed. T. B., & Das, A. (1988). Handbook of biomass downdraft gasifier engine systems. Solar Energy Research Institute. https://www.nrel.gov/docs/legosti/old/3022.pdf

26. REN21. (2021). Renewables 2021 Global Status Report, REN21 Secretariat. https://www.ren21.net/wp-content/uploads/2019/05/GSR2021_Full_Report.pdf

27. Salam, A.M., Dhami, A.S., Paul, M.C. (2022). Syngas Production and Combined Heat and Power from Scottish Agricultural Waste Gasification—A Computational Study. Sustainability 2022. 14 (7). 3745. https://doi.org/10.3390/su14073745

28. Şehmus, A., Cengiz, Ö., Fevzi, Y., & Hamit, A. (2011). Effect of n-Butanol Blending with a Blend of Diesel and Biodiesel on Performance and Exhaust Emissions of a Diesel Engine. Industrial & Engineering Chemistry Research, 50(15). 8803-9478 https://doi.org/10.1021/ie201023f

29. Shivpal V, Addrei M. D., Vinay, K., Preeti, C. B., Nawaz, K., Anuradha S., Xinwei S., Raveendran S., Parameswaran B., Zengqiang Z., Ashok P., Mukesh K. A., & Mukesh, K. A. (2023) Reaction engineering during biomass gasification and conversion to energy. Energy, 266, 126458. https://doi.org/10.1016/j.energy.2022.126458

30. Siedlecki, M., Jong, W.D., & Verkooijen, A.H.M. (2011). Fluidized Bed Gasification as a Mature and Reliable Technology for the Production of Bio-Syngas and Applied in the Production of Liquid Transportation Fuels—A Review, Energies 2011, 4(3), 389-434. https://doi.org/10.3390/en4030389

31. Sittisun, P., Tippayawong, N., & Shimpalee, S. (2019). Gasification of Pelletized Corn Residues with Oxygen Enriched Air and Steam. International Journal of Renewable Energy Development, 8(3), 215-224. https://doi.org/10.14710/ijred.8.3.215-224

32. Smail, B., & Mohiuddin, AKM. (2020). Combustion Chamber Design Effect on The Rotary Engine Performance- A Review. International Journal of Automotive Engineering, 11(4), 200-212. https://doi.org/10.20485/jsaeijae.11.4_200

33. Speight, J.G. (2015). Handbook of Coal Analysis, John Wiley & Sons, Inc. https://onlinelibrary.wiley.com/doi/book/10.1002/9781119037699

34. Toonssen, R., Sollai, S., Aravind, P., Woudstra, N. & Verkooijen, A. H. (2011). Alternative system designs of biomass gasification SOFC/GT hybrid systems. International journal of hydrogen energy, 36(16), 10414-10425. https://doi.org/10.1016/j.ijhydene.2010.06.069

35. United Nations, Department of Economic and Social Affairs, Population Division (2022).World Population Prospects 2022: Ten Key Messages.https://www.un.org/development/desa/pd/sites/www.un.org.development.desa.pd/files/undesa_pd_2022_wpp_key-messages.pdf

36. Voća, N, Bilandžija, N., Jurišić, V., Matin, A., Krička, T., & Sedak, I. (2016). Proximate, Ultimate, and Energy Values Analysis of Plum Biomass By-products Case Study: Croatia's Potential. Journal of Agricultural Science and Technology, 18 (6),1655-1666, https://jast.modares.ac.ir/article-23-11653-en.pdf

37. Wankel Supertec GmbH. (2022). "About Wankel Rotary Engines." https://www.wankelsupertec.de/en_rotary_engines.html. Accessed on 22nd April 2022

38. World Bioenergy Association. (WBA) (2021), Global Bioenergy Statistics 2021. https://www.worldbioenergy.org/uploads/211214%20WBA%20GBS%202021.pdf

39. Zeba H, M.R. Ravi & Sangeeta K (2022) Modelling and simulation of downdraft biomass gasifier: Issues and challenges. Biomass and Bioenergy, 162, 106483. https://doi.org/10.1016/j.biombioe.2022.106483